

UC Davis

UC Davis Previously Published Works

Title

Non-Invasive Compression-Induced Anterior Cruciate Ligament (ACL) Injury and In Vivo Imaging of Protease Activity in Mice.

Permalink

<https://escholarship.org/uc/item/40g0b4xv>

Authors

Christiansen, Blaine

Lin, Yu-Yang

Publication Date

2023-09-29

DOI

10.3791/65249

Peer reviewed



Non-Invasive Compression-Induced ACL Injury and *In Vivo* Imaging of Protease Activity in Mice

Yu-Yang Lin,

Blaine A. Christiansen

University of California Davis Health, Department of Orthopaedic Surgery, Lawrence J. Ellison Musculoskeletal Research Center, 2700 Stockton Blvd, Suite 2301, Sacramento, CA 95817

Abstract

Traumatic joint injuries such as anterior cruciate ligament (ACL) rupture or meniscus tears commonly lead to post-traumatic osteoarthritis (PTOA) within 10–20 years following injury. Understanding the early biological processes initiated by joint injuries (e.g., inflammation, matrix metalloproteinases (MMPs), cathepsin proteases, bone resorption) is crucial for understanding the etiology of PTOA. However, there are few options for *in vivo* measurement of these biological processes, and the early biological responses may be confounded if invasive surgical techniques or injections are used to initiate OA. In our studies of PTOA, we have used commercially available near-infrared protease activatable probes combined with fluorescence reflectance imaging (FRI) to quantify protease activity *in vivo* following non-invasive compression-induced ACL injury in mice. This non-invasive ACL injury method closely recapitulates clinically relevant injury conditions and is completely aseptic since it does not involve disrupting the skin or the joint capsule. The combination of these injury and imaging methods allows us to study the time course of protease activity at multiple time points following a traumatic joint injury.

SUMMARY:

Non-invasive ACL injury is a reliable and clinically relevant method for initiating post-traumatic osteoarthritis (PTOA) in mice. This injury method also allows for *in vivo* quantification of protease activity in the joint at early time points post-injury using protease-activatable near infrared probes and fluorescence reflectance imaging.

INTRODUCTION:

Osteoarthritis is a pervasive health issue that affects millions of people in the United States¹. Post-traumatic osteoarthritis (PTOA) is a subset of OA that is initiated by a joint injury such as anterior cruciate ligament (ACL) rupture, meniscus injury, or intra-articular fracture². The

Corresponding Author: Blaine A. Christiansen, University of California Davis Health, Department of Orthopaedic Surgery, Lawrence J. Ellison Musculoskeletal Research Center, 2700 Stockton Blvd, Suite 2301, Sacramento, CA 95817, *Phone:* 916-734-3974, *bchristiansen@ucdavis.edu.*

A complete version of this article that includes the video component is available at <http://dx.doi.org/10.3791/65249>.

DISCLOSURES:

The authors have nothing to disclose.

proportion of symptomatic OA patients that can be classified as PTOA is at least 12%³, and this etiology typically affects a younger population than idiopathic OA⁴. Mouse models of OA are crucial tools for investigating disease etiology and potential OA treatments on a much shorter timeline (4–12 weeks in mouse models compared to 10–20 years in humans). However, the methods to initiate OA in mice commonly involve invasive surgical techniques such as ACL transection^{5,6}, removal or destabilization of the medial meniscus^{5,7–16}, or a combination of the two^{17–19}, which do not reproduce clinically relevant injury conditions. Surgical models also exacerbate inflammation in the joint due to disruption of the joint capsule, which could accelerate OA progression.

Non-invasive knee injury mouse models provide the opportunity to study biological and biomechanical changes at early time points post-injury and may yield more clinically relevant results²⁰. Our lab has established a non-invasive injury model that uses a single externally applied tibial compression overload to induce anterior cruciate ligament (ACL) rupture in mice^{21–24}. This non-invasive injury method is able to produce an aseptic joint injury without disrupting the skin or joint capsule.

Fluorescence reflectance imaging (FRI) is an optical imaging method that involves exciting a target with infrared light at a specific wavelength and quantifying the reflected light emitted at another wavelength. Commercially available protease-specific probes can be injected into animal models and FRI can then be used to quantify protease activity at specific sites such as the knee joint. This method has been widely used for *in vivo* detection of biological activities such as inflammation. The probes used for this application are fluorescently quenched until they encounter relevant proteases. Those proteases will then break an enzyme cleavage site on the probes after which they will produce a near-infrared fluorescent signal. These probes and this imaging method have been extensively validated and used in studies of cancer^{25–28} and atherosclerosis^{29–32}, and our group has used them for studies of the musculoskeletal system to measure markers of inflammation and matrix degradation^{23,24,33}.

Together, non-invasive joint injury combined with *in vivo* FRI and protease activatable probes provide a unique ability to track inflammation and protease activity following a traumatic joint injury. This analysis can be done as early as hours or even minutes after injury, and the same animal can be assessed multiple times to study the time course of protease activity in the joint. Importantly, this imaging method may not be feasible when combined with surgical models of OA, since disruption of the skin and joint capsule results in a fluorescence signal that would confound the signal from within the joint.

PROTOCOL:

All procedures described have been approved by the Institutional Animal Care and Use Committee at the University of California Davis.

Non-Invasive ACL Injury

ACL injury produced by an externally applied compressive load is a simple and reproducible method that closely recapitulates ACL injury conditions in humans. This protocol is written for the ElectroForce 3200 system but could be adapted for similar systems.

Procedure:

1. Open the WinTest software and select an existing control file or create a new file.
2. Turn on the power to the actuator.
3. In calibration menu, tare the force reading of the load cell and set the displacement of the actuator to '0'.
4. Use 1–4% inhaled isoflurane in oxygen to anesthetize animals and ensure the mice are fully anesthetized by toe pinch and/or tail pinch.
5. Place the mouse in a prone position on the platform. Position the lower leg vertically between two loading fixtures (Fig. 1). Fit the foot into the cutout of the top fixture and the knee in the cup of the bottom fixture.
6. Manually adjust the height of bottom fixture to apply a preload of 1–2 N (monitored in real time on the computer screen) and tighten the set screw to hold the position. The preload is necessary to hold the leg in the correct position prior to applying the injury load.
7. Apply a single compressive load to a target force (~12–15 N) or target displacement (~1.5–2.0 mm). Applying the load at a slower loading rate (~1 mm/s) will provide a greater level of real-time monitoring and control but will likely result in an avulsion failure of the ACL. Applying a faster loading rate (~200 mm/s) will be more likely to produce a mid-substance ACL injury²². The loading rate can be set in the software control file and confirmed using the force-displacement data.

NOTE: Bone fracture during tibial compression loading is typically not a concern since the fracture force (~20 N) is considerably higher than the ACL injury force. However, this should be monitored with palpation, and imaging (i.e., x-ray) can be used to confirm that no tibial fractures have occurred.

8. Injury is typically indicated with a sound (“click” or “crunch”) and a release of force that is identifiable on the force-displacement plots (Fig. 1(c)). If a slower loading rate is used, the compressive load should be stopped immediately after injury to prevent further loading and possible damage to other joint tissues.

NOTE: ACL injury typically occurs at 8–15 N depending on body mass³⁴. It is important to set a target force greater than the anticipated ACL injury force.

9. ACL injury can be confirmed using an anterior-posterior drawer test^{35,36} or comparable assessment of joint instability.
10. Administer an animal weight-dependent dose (0.1 mg/kg) of analgesic (buprenorphine) to mice post-injury.

Fluorescence Reflectance Imaging (FRI)

1. Mice Fur Removal—For optical imaging, animal fur (particularly dark fur) is highly effective at blocking, absorbing, and scattering light, therefore fur must be removed as much as possible from the area around the knee joints before imaging. A depilatory cream is typically more effective for fur removal than clippers. Nude or hairless mice don't require fur removal. However, for most commonly used mouse strains (e.g., C57BL/6) fur removal is necessary. If possible, feed mice with low-fluorescence food before imaging (e.g., Teklad Diets, TD.94045, AIN-93G Purified Diet, Envigo, Indianapolis, IN). Standard mouse chow contains chlorophyll which auto-fluoresces with a wavelength around 700 nm and may affect data collection from the near-infrared FRI system.

Procedure:

- 1.1** Anesthetize mice with 1–4% inhaled isoflurane in oxygen. Keep mice on a heating pad as much as possible and apply eye ointment to prevent irritation of the eyes.
- 1.2** Use a cotton swab to apply depilatory cream onto the anterior (cranial) aspect of the legs of the mice around the knee joint.
- 1.3** Let the cream stand for ~1 minute, then use wipes to remove the cream and fur from the leg. Repeat if necessary.
- 1.4** Once the knee joints are fully exposed without any fur covering the area, clean the legs with alcohol wipes to remove any remaining depilatory cream.

NOTE: Depilatory cream can be used on the same mice multiple times throughout a study, but these applications should be at least one week apart to prevent unnecessary irritation of the skin.

2. Preparation of the Probe Solution—Procedure:

- 2.1** If necessary, dilute the fluorescence activatable probe according to the manufacturer's instructions in sterile 1x phosphate buffered saline (PBS). One vial of the commercially available probe (see Table of Materials) typically contains 20 nmol in 0.15 mL 1 × PBS. To dilute the solution in the vial, add 1.35 mL of 1 × PBS to make 20 nmol in 1.5 mL 1 × PBS.

NOTE: After dilution, one vial can be used to image 10 mice when injecting 0.15 mL per mouse.

- 2.2** Vortex the solution with a minimum speed set of "5" (~2000 RPM) for 30s to ensure that the probe is dissolved in solution and then centrifuge briefly to ensure that all liquid is out of the lid.
- 2.3** The solution can be stored at 2–8° C in a location that is protected from light for up to 12 months.

3. Retro-Orbital Injection³⁷—Procedure:

- 3.1 Use 1–4% inhaled isoflurane in oxygen to anesthetize mice and place the mouse on its side with the snout in a nose cone.
- 3.2 Use ~29G insulin syringes for injection of probe solution
- 3.3 Keep the syringe covered before use to prevent exposure to light.
- 3.4 When doing injection:
 - 3.4.1 The injection should be administered on the inside of the eye (lacrimal caruncula), and the bevel of the syringe should be angled towards the eye. For right-handed people, it is recommended to inject into the right eye of the mouse with the animal facing right.
 - 3.4.2 With the non-injecting hand, gently pull back the skin around the eye to stabilize the head and cause the eye to protrude.
 - 3.4.3 Angle the syringe parallel to the body of the mouse.
 - 3.4.4 Gently advance the syringe past the eye until it meets rigid resistance, do not attempt to push past this point.
 - 3.4.5 Slowly inject the probe solution into the retro-orbital sinus, then slowly pull the needle out of the eye socket. If no solution comes out with the needle, the injection was successful.
 - 3.4.6 Apply saline or eye ointment to the injected eye.

NOTE: Based on the documentation provided with the imaging probes, the optimal imaging time is typically between 1 and 2 days after injection of the probe solution. If possible, it is recommended to do an initial time screening to determine the optimal imaging time for each specific application.

NOTE: Mice will metabolize the injected probe within approximately 7 days, after which a new dose of probe solution will need to be injected if additional time points are desired.

4. Fluorescence Reflectance Imaging—The procedures in this section are specific to the IVIS Spectrum Imaging System. Similar imaging can be performed with comparable systems.

Procedure:

- 4.1 Anesthetize mice with 1–4% inhaled isoflurane in oxygen and place supine in the imaging system with the snout in a nose cone.
- 4.2 Position the mouse with the lower legs extended so that the knees are pointed slightly in the air (it may be necessary to tape down the feet). It is critical that a consistent positioning is used for all animals.
- 4.3 Opening the Living Image software on the imaging system computer; the Living Image IVIS Acquisition Control Panel will appear.

- 4.4 To warm up the system, click 'Initialize' and wait until the temperature light turns green.
- 4.5 Click 'Imaging Wizard' and the Imaging Wizard window will appear.
- 4.6 Click 'Filter Pair', and make sure the setting is on 'Epi-Illumination', then press 'Next'.
- 4.7 To select the correct excitation/emission settings, find your probe of interest from the pulldown list. If you can't find the correct probe, find the Name 'Input Ex/Em' and manually type in the value of Excitation Peak and Emission Peak based on the property of the probe that you use (e.g., for Excitation Peak, enter 675, and for Emission Peak, enter 720). Click 'Next'.
- 4.8 Choose 'Mouse' for Imaging Subject. In Exposure Parameters, make sure the 'Auto Settings' is checked, and the 'Fluorescent' and 'Photograph' options should be both selected. Select 'D – 22.6 cm' in the checklist of Field of View. Press 'Next'.
- 4.9 Imaging setting can be seen and modified on the right panel of the IVIS Acquisition Control Panel. Make sure that all settings are correct and then press the 'Acquire Sequence' button. After the image shows up, confirm that the image had adequate exposure. If not, change the exposure time setting and click 'Acquire Sequence' again.
- 4.10 To analyze the image, position a region of interest (ROI) circle with consistent size over each knee joint on the black and white image (this prevents biased positioning based on areas of fluorescent signal). Calculate total radiant efficiency and/or average radiant efficiency for each knee joint. If the radiant efficiency is also calculated on the contralateral legs, the data can be normalized by dividing the radiant efficiency measurement for the injured leg by the radiant efficiency measurement of the contralateral leg.

NOTE: If a region of interest with consistent area is used for all knees, both total radiant efficiency and average radiant efficiency will yield similar results. If regions of interest with different sizes are used, using average radiant efficiency is recommended.

NOTE: Normalizing radiant efficiency data from the injured joint by the data from the uninjured contralateral knee will provide an internal control to account for any differences in the amount of probe injected and the delivery efficiency between different animals.

REPRESENTATIVE RESULTS:

After applying a single compressive force (1 mm/s until injury) on the lower legs of 3-month-old male C57BL/6J mice, ACL injury was consistently induced in all mice. The average compressive force at knee injury was approximately 10 N (Figure 1).

FRI analysis showed significantly greater protease activity in the injured joints of mice subjected to non-invasive ACL injury at 7 days following injury (Figure 2). We also performed FRI analysis of knee joints from mice that underwent surgical stabilization of the knee joint immediately after non-invasive ACL injury, similar to what has been previously described in rats^{35,36,38}. This analysis showed considerably greater fluorescent signal in mice that were subjected to stabilization surgery compared to mice that did not have surgery at both 2 and 4 weeks post-injury. These data suggest that invasive surgical procedures can confound the analysis of protease activity in the joint.

DISCUSSION:

Our lab has established and rigorously described a reproducible non-invasive method for inducing ACL injury in mice^{20,21,24,33}. This simple and efficient injury method can be performed in just a few minutes, which facilitates high-throughput studies of PTOA. This injury method also closely recapitulates injury conditions relevant to human ACL injury. Surgical methods used to induce OA in mice may preclude the use of in vivo imaging methods to measure the time course and magnitude of protease activity in the joint following injury. In contrast, non-invasive OA mouse models (reviewed in²⁰) combined with FRI provide a unique capability for in vivo imaging of protease activity in mouse knee joints following injury.

The inflammatory response following injury is critically important in OA progression. However, the methods used to analyze inflammation in the joint are typically expensive, time-consuming, and destructive. For example, techniques such as reverse transcription polymerase chain reaction (RT-PCR) or RNAseq can be used to quantify a wide array of genes in whole joints, individual tissues, or single cells. However, this method requires mice to be euthanized to acquire injured and uninjured knee joints. These mice cannot be analyzed at multiple time points such as an early time point during the peak protease response (i.e. 3–14 days after injury) and a later time point when OA is more severe (i.e., 4–6 weeks after injury). In contrast, FRI combined with non-invasive joint injury provides the ability to analyze protease activity at multiple time points in the knee joints of mice in vivo³⁹. This allows for longitudinal analysis of the same mice and makes FRI a relatively lower cost outcome than RT-PCR or RNAseq. In addition, multiple probes or targets can be imaged simultaneously at different wavelengths, which can provide multiple results for different purposes. Measuring protease activity in the joint using FRI does not provide a rigorous quantification of all inflammatory processes that occur during OA progression, but the in vivo and longitudinal data provided by this method may still be useful for tracking the magnitude and time course of inflammatory protease activity following joint injury.

The fluorescence activatable probe solution used for FRI imaging of protease activity must be delivered intravenously (IV). The most common ways to perform IV injection in mice is tail vein injection and retro-orbital injection. Retro-orbital injection is often easier to perform and more easily facilitates the necessary injection volume than tail vein injection. Literature also indicates that retro-orbital delivery may cause less stress to mice with no difference in drug delivery or efficacy compared to the tail vein injection⁴⁰. These findings

suggest that retro-orbital injection is suitable for injection of the fluorescence activatable probe solution for FRI imaging.

The resolution of FRI is relatively low compared to some other imaging techniques, but the quantitative results can provide sufficient information on the time course and magnitude of the inflammatory protease response during OA progression. A limitation of this technique is that tissue autofluorescence could affect the results, but this problem can be solved with a thorough plan before the experiment (probe type, strain of mice, animal positioning, etc.). Unlike other preclinical imaging methods (e.g., microPET, microSPECT, microCT, MRI), FRI is not able to be directly translated to a clinical imaging modality due to the drastic differences in size between mice and humans, since the depth of light penetration is limited. However, in preclinical studies using rodent models, the knee joint is close to the skin with minimal soft tissue coverage. Consequently, FRI is an effective tool for detecting protease activity in the knee joint of mice.

In conclusion, non-invasive ACL injury provides a simple and reproducible method to initiate PTOA in mice. This injury method also facilitates the use of protease-activatable probes and Fluorescence Reflectance Imaging for in vivo measurement of the time course and magnitude of inflammatory protease activity in mouse joints during OA progression. Future studies could use these techniques and the multiple commercially available near-infrared fluorescence activatable probes to investigate mechanisms of OA progression in mice with different ages, sexes, and genetic backgrounds or to evaluate potential therapies for slowing or preventing OA progression after joint injury.

ACKNOWLEDGMENTS:

Research reported in this publication was supported by the National Institute of Arthritis and Musculoskeletal and Skin Diseases, part of the National Institutes of Health, under Award Number R01 AR075013.

REFERENCES:

1. Deshpande BR et al. Number of Persons With Symptomatic Knee Osteoarthritis in the US: Impact of Race and Ethnicity, Age, Sex, and Obesity. *Arthritis Care Res (Hoboken)*. 68 (12), 1743–1750, doi:10.1002/acr.22897, (2016). [PubMed: 27014966]
2. Carbone A & Rodeo S Review of current understanding of post-traumatic osteoarthritis resulting from sports injuries. *J Orthop Res*. 35 (3), 397–405, doi:10.1002/jor.23341, (2017). [PubMed: 27306867]
3. Thomas AC, Hubbard-Turner T, Wikstrom EA & Palmieri-Smith RM Epidemiology of Posttraumatic Osteoarthritis. *J Athl Train*. 52 (6), 491–496, doi:10.4085/1062-6050-51.5.08, (2017). [PubMed: 27145096]
4. Wang LJ, Zeng N, Yan ZP, Li JT & Ni GX Post-traumatic osteoarthritis following ACL injury. *Arthritis Res Ther*. 22 (1), 57, doi:10.1186/s13075-020-02156-5, (2020). [PubMed: 32209130]
5. Glasson SS, Blanchet TJ & Morris EA The surgical destabilization of the medial meniscus (DMM) model of osteoarthritis in the 129/SvEv mouse. *Osteoarthritis Cartilage*. 15 (9), 1061–1069, doi:S1063-4584(07)00110-0 [pii] 10.1016/j.joca.2007.03.006, (2007). [PubMed: 17470400]
6. Kamekura S et al. Osteoarthritis development in novel experimental mouse models induced by knee joint instability. *Osteoarthritis Cartilage*. 13 (7), 632–641, doi:S1063-4584(05)00077-4 [pii] 10.1016/j.joca.2005.03.004, (2005). [PubMed: 15896985]

7. Ma HL et al. Osteoarthritis severity is sex dependent in a surgical mouse model. *Osteoarthritis Cartilage*. 15 (6), 695–700, doi:S1063–4584(06)00324–4 [pii] 10.1016/j.joca.2006.11.005, (2007). [PubMed: 17207643]
8. Malfait AM et al. ADAMTS-5 deficient mice do not develop mechanical allodynia associated with osteoarthritis following medial meniscal destabilization. *Osteoarthritis Cartilage*. 18 (4), 572–580, doi:S1063–4584(09)00319–7 [pii] 10.1016/j.joca.2009.11.013, (2010). [PubMed: 20036347]
9. Yang S et al. Hypoxia-inducible factor-2alpha is a catabolic regulator of osteoarthritic cartilage destruction. *Nat Med*. 16 (6), 687–693, doi:nm.2153 [pii] 10.1038/nm.2153, (2010). [PubMed: 20495569]
10. Moodie JP, Stok KS, Muller R, Vincent TL & Shefelbine SJ Multimodal imaging demonstrates concomitant changes in bone and cartilage after destabilisation of the medial meniscus and increased joint laxity. *Osteoarthritis Cartilage*. 19 (2), 163–170, doi:S1063–4584(10)00391–2 [pii] 10.1016/j.joca.2010.11.006, (2011). [PubMed: 21094262]
11. Li J et al. Knockout of ADAMTS5 does not eliminate cartilage aggrecanase activity but abrogates joint fibrosis and promotes cartilage aggrecan deposition in murine osteoarthritis models. *J Orthop Res*. 29 (4), 516–522, doi:10.1002/jor.21215, (2011). [PubMed: 21337391]
12. Shapiro F & Glimcher MJ Induction of osteoarthritis in the rabbit knee joint. *Clin Orthop Relat Res*. (147), 287–295 (1980). [PubMed: 6154558]
13. Meacock SC, Bodmer JL & Billingham ME Experimental osteoarthritis in guinea-pigs. *J Exp Pathol (Oxford)*. 71 (2), 279–293 (1990). [PubMed: 2331410]
14. Armstrong SJ, Read RA, Ghosh P & Wilson DM Moderate exercise exacerbates the osteoarthritic lesions produced in cartilage by meniscectomy: a morphological study. *Osteoarthritis Cartilage*. 1 (2), 89–96, doi:S1063–4584(05)80023–8 [pii], (1993). [PubMed: 8886084]
15. Pastoureau P, Leduc S, Chomel A & De Ceuninck F Quantitative assessment of articular cartilage and subchondral bone histology in the meniscectomized guinea pig model of osteoarthritis. *Osteoarthritis Cartilage*. 11 (6), 412–423, doi:10.1016/s1063-4584(03)00050-5, (2003). [PubMed: 12801481]
16. Wancket LM et al. Anatomical localization of cartilage degradation markers in a surgically induced rat osteoarthritis model. *Toxicol Pathol*. 33 (4), 484–489, doi:10.1080/01926230590965364, (2005). [PubMed: 16036866]
17. Karahan S, Kincaid SA, Kammermann JR & Wright JC Evaluation of the rat stifle joint after transection of the cranial cruciate ligament and partial medial meniscectomy. *Comp Med*. 51 (6), 504–512 (2001). [PubMed: 11924812]
18. Kamekura S et al. Osteoarthritis development in novel experimental mouse models induced by knee joint instability. *Osteoarthritis and cartilage / OARS, Osteoarthritis Research Society*. 13 (7), 632–641, doi:10.1016/j.joca.2005.03.004, (2005).
19. Jones MD et al. In vivo microfocal computed tomography and micro-magnetic resonance imaging evaluation of antiresorptive and antiinflammatory drugs as preventive treatments of osteoarthritis in the rat. *Arthritis Rheum*. 62 (9), 2726–2735, doi:10.1002/art.27595, (2010). [PubMed: 20533290]
20. Christiansen BA et al. Non-invasive mouse models of post-traumatic osteoarthritis. *Osteoarthritis Cartilage*. 23 (10), 1627–1638, doi:10.1016/j.joca.2015.05.009, (2015). [PubMed: 26003950]
21. Christiansen BA et al. Musculoskeletal changes following non-invasive knee injury using a novel mouse model of post-traumatic osteoarthritis. *Osteoarthritis Cartilage*. 20 (7), 773–782, doi:10.1016/j.joca.2012.04.014, (2012). [PubMed: 22531459]
22. Lockwood KA, Chu BT, Anderson MJ, Haudenschild DR & Christiansen BA Comparison of loading rate-dependent injury modes in a murine model of post-traumatic osteoarthritis. *J Orthop Res*. 32 (1), 79–88, doi:10.1002/jor.22480, (2014). [PubMed: 24019199]
23. Satkunanathan PB et al. In vivo fluorescence reflectance imaging of protease activity in a mouse model of post-traumatic osteoarthritis. *Osteoarthritis Cartilage*. 22 (10), 1461–1469, doi:10.1016/j.joca.2014.07.011, (2014). [PubMed: 25278057]
24. Hsia AW et al. Post-traumatic osteoarthritis progression is diminished by early mechanical unloading and anti-inflammatory treatment in mice. *Osteoarthritis Cartilage*. 29 (12), 1709–1719, doi:10.1016/j.joca.2021.09.014, (2021). [PubMed: 34653605]

25. Zhang H et al. Biochromoendoscopy: molecular imaging with capsule endoscopy for detection of adenomas of the GI tract. *Gastrointest Endosc.* 68 (3), 520–527, doi:S0016–5107(08)00228–9 [pii] 10.1016/j.gie.2008.02.023, (2008). [PubMed: 18499106]
26. Gounaris E et al. Live imaging of cysteine-cathepsin activity reveals dynamics of focal inflammation, angiogenesis, and polyp growth. *PLoS One.* 3 (8), e2916, doi:10.1371/journal.pone.0002916, (2008). [PubMed: 18698347]
27. Sheth RA & Mahmood U Optical molecular imaging and its emerging role in colorectal cancer. *Am J Physiol Gastrointest Liver Physiol.* 299 (4), G807–820, doi:ajpgi.00195.2010 [pii] 10.1152/ajpgi.00195.2010, (2010). [PubMed: 20595618]
28. Clapper ML et al. Detection of colorectal adenomas using a bioactivatable probe specific for matrix metalloproteinase activity. *Neoplasia.* 13 (8), 685–691 (2011). [PubMed: 21847360]
29. Nahrendorf M et al. Dual channel optical tomographic imaging of leukocyte recruitment and protease activity in the healing myocardial infarct. *Circ Res.* 100 (8), 1218–1225, doi:01.RES.0000265064.46075.31 [pii] 10.1161/01.RES.0000265064.46075.31, (2007). [PubMed: 17379832]
30. Jaffer FA et al. Optical visualization of cathepsin K activity in atherosclerosis with a novel, protease-activatable fluorescence sensor. *Circulation.* 115 (17), 2292–2298, doi:CIRCULATIONAHA.106.660340 [pii] 10.1161/CIRCULATIONAHA.106.660340, (2007). [PubMed: 17420353]
31. Jaffer FA, Libby P & Weissleder R Optical and multimodality molecular imaging: insights into atherosclerosis. *Arterioscler Thromb Vasc Biol.* 29 (7), 1017–1024, doi:ATVBAHA.108.165530 [pii] 10.1161/ATVBAHA.108.165530, (2009). [PubMed: 19359659]
32. Razansky D et al. Multispectral optoacoustic tomography of matrix metalloproteinase activity in vulnerable human carotid plaques. *Mol Imaging Biol.* 14 (3), 277–285, doi:10.1007/s11307-011-0502-6, (2012). [PubMed: 21720908]
33. Hsia AW et al. Osteophytes and fracture calluses share developmental milestones and are diminished by unloading. *J Orthop Res.* 36 (2), 699–710, doi:10.1002/jor.23779, (2018). [PubMed: 29058776]
34. Blaker CL, Little CB & Clarke EC Joint loads resulting in ACL rupture: Effects of age, sex, and body mass on injury load and mode of failure in a mouse model. *J Orthop Res.* 35 (8), 1754–1763, doi:10.1002/jor.23418, (2017). [PubMed: 27601010]
35. Murata K et al. Controlling joint instability delays the degeneration of articular cartilage in a rat model. *Osteoarthritis Cartilage.* 25 (2), 297–308, doi:10.1016/j.joca.2016.10.011, (2017). [PubMed: 27756697]
36. Murata K et al. Controlling Abnormal Joint Movement Inhibits Response of Osteophyte Formation. *Cartilage.* 9 (4), 391–401, doi:10.1177/1947603517700955, (2018). [PubMed: 28397529]
37. Yardeni T, Eckhaus M, Morris HD, Huizing M & Hoogstraten-Miller S Retro-orbital injections in mice. *Lab Anim (NY).* 40 (5), 155–160, doi:10.1038/labani0511-155, (2011). [PubMed: 21508954]
38. Kokubun T et al. Effect of Changing the Joint Kinematics of Knees With a Ruptured Anterior Cruciate Ligament on the Molecular Biological Responses and Spontaneous Healing in a Rat Model. *Am J Sports Med.* 44 (11), 2900–2910, doi:10.1177/0363546516654687, (2016). [PubMed: 27507845]
39. Bhatti FU et al. Characterization of Non-Invasively Induced Post-Traumatic Osteoarthritis in Mice. *Antioxidants (Basel).* 11 (9), doi:10.3390/antiox11091783, (2022).
40. Steel CD, Stephens AL, Hahto SM, Singletary SJ & Ciavarra RP Comparison of the lateral tail vein and the retro-orbital venous sinus as routes of intravenous drug delivery in a transgenic mouse model. *Lab Anim (NY).* 37 (1), 26–32, doi:10.1038/labani0108-26, (2008). [PubMed: 18094699]

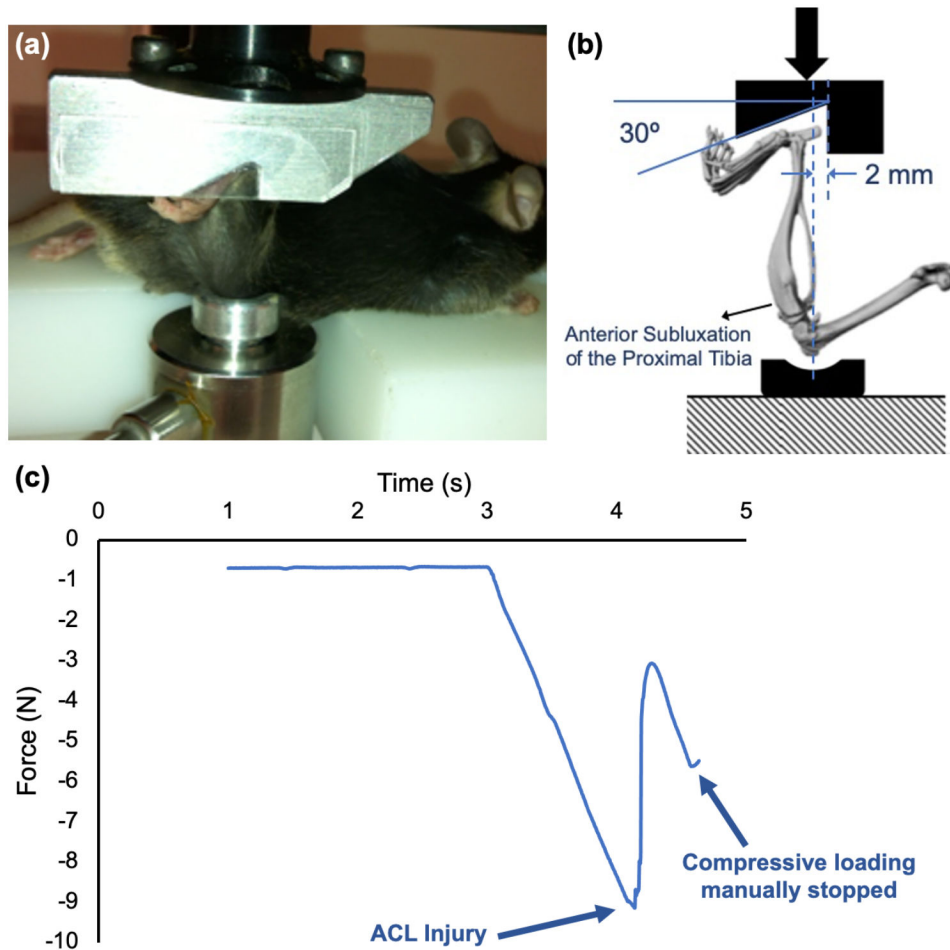


Figure 1: Non-invasive ACL injury setup and a force-time plot during injury.

(A-B) The mouse's lower leg is positioned vertically in the system, with the ankle placed in a notch of the top fixture and the knee joint placed in a shallow cup on the bottom fixture. The bottom fixture is locked into place with a set screw after manually applying a preload of 1–2 N. (C) Force-displacement plot, which shows ACL injury at approximately 9 N.

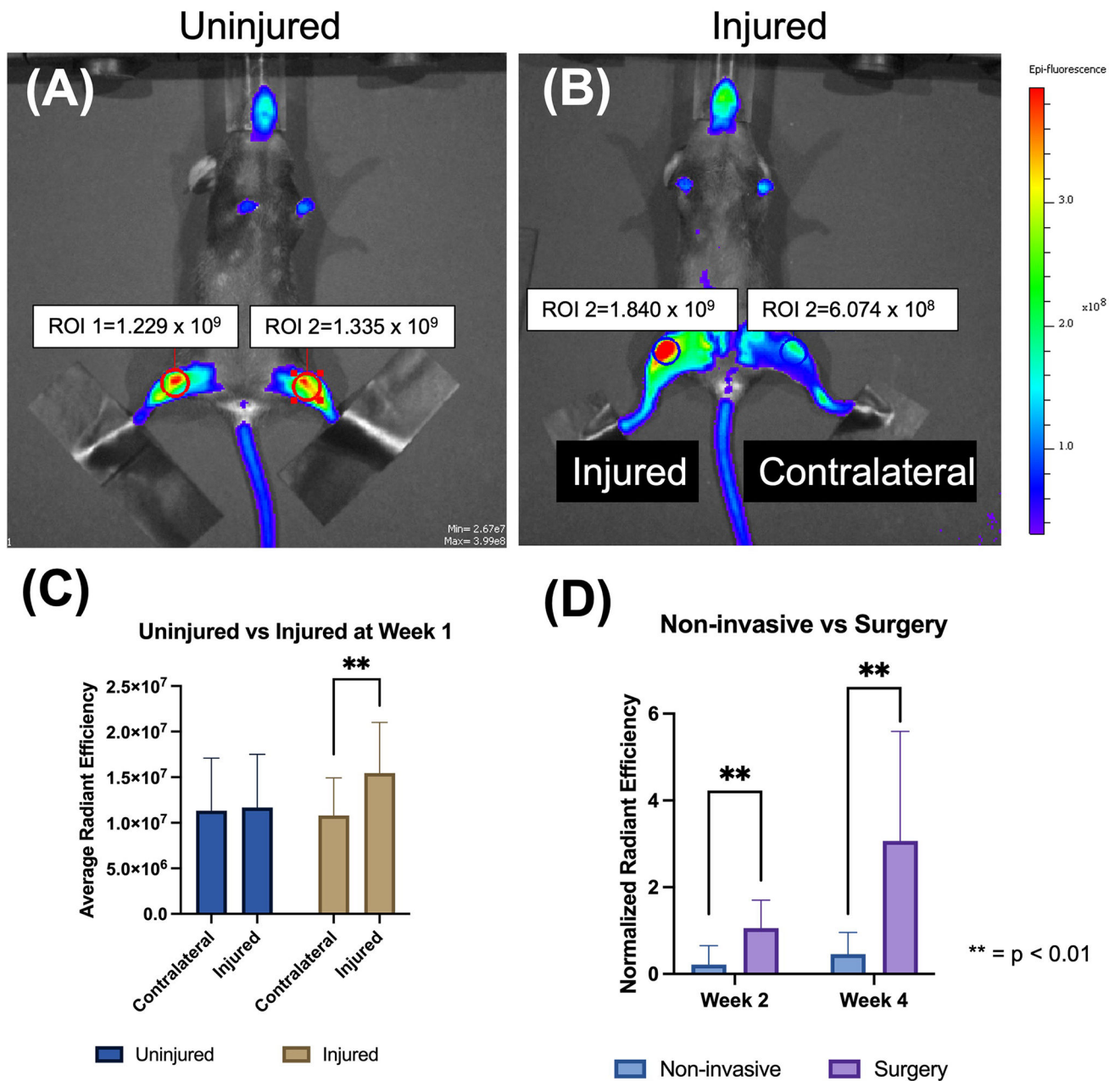


Figure 2: Fluorescence Reflectance Imaging detecting protease activity in mouse knee joints. (A-B) Representative images of uninjured (A) and injured (B) mice following injury. (C) Average radiant efficiency of both knee joints for uninjured and injured mice one week following non-invasive ACL injury. Injured joints showed 43% greater average radiant efficiency compared to contralateral joints and joints from uninjured mice. (D) Normalized total radiant efficiency (R/L) for non-invasively injured mice and injured mice that were also subjected to joint restabilization surgery. We commonly observe a ~30–80% greater radiant efficiency in injured joints compared to contralateral joints at 1–4 weeks post-injury.

In contrast, surgically operated joints exhibited ~300% greater radiant efficiency at week 4 compared to contralateral joints, suggesting a notable confounding effect of surgery.

Author Manuscript

Author Manuscript

Author Manuscript

Author Manuscript

Table of Materials

| Name of Material/ Equipment | Company | Catalog Number | Comments/Description |
|-------------------------------|------------------------------|----------------|---|
| Materials testing systems | TA Instruments | | Electroforce 3200 or equivalent |
| Uniaxial load cell | TA Instruments | | 20 N capacity |
| Fixtures | | | Custom-made knee fixture, ankle fixture, and platform |
| Air Anesthesia System | | | Isoflurane vaporizer with induction chamber and nose cone |
| Buprenorphine | | | Analgesic post-injury |
| IVIS Spectrum | Perkin Elmer | 124262 | Can also use comparable optical imaging system |
| ProSense680 | Perkin Elmer | NEV10003 | Can also use other probes such as OsteoSense, MMPSense, Cat K, AngioSense, etc. |
| Depilatory Cream | Veet | B001KYPZ4G | or equivalent |
| Vortex-Genie 2 | Scientific Industries, Inc. | SI-0236 | or equivalent |
| 10x Phosphate-Buffered Saline | Tissue Protech | PBS01-32R | or equivalent |
| Kimwipes | Kimberly-Clark Corporation | 06-666 | or equivalent |
| Sterile Syringe with Needle | Spectrum Chemical Mfg. Corp. | 550-82231-CS | Covidien 1 mL TB Syringe with 28G × 1/2 in. Needle, Sterile or equivalent |